Caught in the Act: ATP hydrolysis of an ABC-multidrug transporter followed by real-time magic angle spinning NMR

Ute A. Hellmich[a], Winfried Haase[b], Saroj Velamakanni[c],
Hendrik W. van Veen[c], Clemens Glaubitz[a,*]

[a] Institute for Biophysical Chemistry, Centre for Biomolecular Magnetic Resonance, Cluster of Excellence Macromolecular Complexes,
J.W. Goethe University, Frankfurt am Main, Germany
[b] Max-Planck-Institute for Biophysics, Frankfurt am Main, Germany
[c] Department of Pharmacology, University of Cambridge, Cambridge, United Kingdom

Abstract The ATP binding cassette (ABC) transporter LmrA from *Lactococcus lactis* transports cytotoxic molecules at the expense of ATP. Molecular and kinetic details of LmrA can be assessed by solid-state nuclear magnetic resonance (ssNMR), if functional reconstitution at a high protein–lipid ratio can be achieved and the kinetic rate constants are small enough. In order to follow ATP hydrolysis directly by ^{31}P-magic angle spinning (MAS) nuclear magnetic resonance (NMR), we generated such conditions by reconstituting LmrA-dK388, a mutant with slower ATP turnover rate, at a protein–lipid ration of 1:150. By analysing time-resolved ^{31}P spectra, protein activity has been directly assessed. These data demonstrate the general possibility to perform ssNMR studies on a fully active full length ABC transporter and also form the foundation for further kinetic studies on LmrA by NMR.
© 2008 Federation of European Biochemical Societies. Published by Elsevier B.V. All rights reserved.

Keywords: Real-time NMR; Solid-state NMR; ABC-transporter; ATP hydrolysis; 31P NMR

1. Introduction

The 64 kDa membrane protein LmrA is a homologue of P-glycoprotein (Pgp), which can confer resistance to chemotherapeutics in cancer patients [1]. ATP binding cassette (ABC)-transporters carry out their specific tasks by utilizing energy released during ATP hydrolysis. Pgp and its bacterial relative LmrA use this energy in order to transport lipophilic substrates through the membrane. All ABC-transporters have a similar domain architecture comprising of two transmembrane domains (TMDs) and two nucleotide binding domains (NBDs). These domains can either be encoded on a single polypeptide chain or as separate proteins. LmrA is a homodimer with one TMD and one NBD fused into a single polypeptide [2]. The NBDs contain the signature motifs that define the membership of a protein to the ABC-superfamily, the Walker A and Walker B domain as well as the C-loop. In this domain, ATP hydrolysis is carried out with the help of the C-loop and the Walker B motif [3].

There has been great progress in structural biology of ABC-transporters, as 11 crystal structures of full-length ABC-transporters are available to date; the vitamin B12 importer BtuCD from *Escherichia coli* [4], the putative multidrug transporter Sav1866 from *Staphylococcus aureus* [5,6], the molybdate/tungsten importer ModBC from *Archaeoglobus fulgidus* [7] and *Methanosarcina acetivorans* [8], the metal-chelate importer HI1470/1 from *Haemophilus influenzae* [9], the lipid flippase/multidrug transporter MsbA from *E. coli*, *Vibrio cholera* and *Salmonella typhimurium* [10], the maltose transporter MalFGK$_2$ from *E. coli* [11] and the methionine uptake transporter MetNI from *E. coli* [12]. In addition, many isolated NBDs at different stages of ATP hydrolysis have been crystallized, reviewed by Oswald et al. [13]. However, neither the structures of full lengths transporters, which represent snapshots of the reaction cycle, nor those of isolated NBDs allow a complete insight into the functional mechanism and the conformational dynamics of a complete ABC-transporter.

Thus, other complementary methods need to be utilized for a meaningful structure-function characterization. Solid-state NMR (ssNMR) offers such a possibility, as the full length transporter can be studied within a lipid environment. So far, studies on ABC-transporters [14] and secondary transporters [15,16] were carried out in substrate–protein equilibrium. In case of ABC transporters, non-hydrolysable ATP analogues have been used in order to emulate a particular state of the catalytic cycle. In contrast, real time ssNMR could provide valuable kinetic data for both transport and catalytic cycle but is challenged due to low sensitivity. However, this problem could be overcome by higher protein concentration and/or triggering and slowing the reaction cycle. Especially the use of ^{31}P nuclear magnetic resonance (NMR) could be usefully as no further isotope labelling of ATP/ADP is required. ^{31}P NMR on a soluble nonspecific nucleoside triphosphatase showed that this approach is generally feasible [17] and kinetic ^{31}P solution NMR studies [18] and saturation transfer experiments on nucleotides [20] in whole *E. coli* cells have been successfully carried out. ^{31}P NMR is mainly used as non-invasive

*Corresponding author. Fax: +49 69 798 29929.
E-mail address: glaubitz@em.uni-frankfurt.de (C. Glaubitz).

Abbreviations: ABC, ATP binding cassette; NMR, nuclear magnetic resonance; ssNMR, solid state NMR; MAS, magic angle spinning; Pgp, P-glycoprotein; TMD, transmembrane domain; NBD, nucleotide binding domain; MD, membrane domain; DDM, *n*-dodecyl-β-ᴅ-maltoside; POPC, 1-palmitoyl-2-oleoyl-*sn*-glycero-3-phosphocholine; POPG, 1-palmitoyl-2-oleoyl-*sn*-glycero-3-[phospho-*rac*-(1-glycerol)]

method to study the metabolism of muscle in vivo as reviewed by Kemp et al. [19]. So far, real time ^{31}P ssNMR has never been used on a purified membrane protein. Real-time measurements of ATP hydrolysis always relied on a fluorescent probe sensitive to the release of inorganic phosphate as shown for actomyosin subfragment 1 ATPase [21]. An assay based on the same fluorescent probe was later employed by He et al. on muscle fibers [22]. This fluorescent probe only detects one component of the ATP hydrolysis reaction, the released inorganic phosphate. The same indirect principle underlies many of the conventional ATPase assays. Either an inorganic complex with free Pi is formed that can be detected colourimetrically, for example by malachite green [23] or molybdate blue [24], or the ATP/ADP ratio or the free Pi is measured using a radioactivity assay after the reaction has been stopped [25]. Alternatively, a subsequent reaction by other enzymes makes use of the released ADP to transform it back into ATP, thereby triggering a second reaction that produces a detectable product, such as NAD$^+$ in the coupled assay that utilize pyruvate kinase and lactate dehydrogenase [26]. ^{31}P NMR on the other hand can be used to measure changes of all phosphorylated compounds directly and simultaneously. Additionally, it allows calculating the ATPase activity of the measured protein as reliably as a conventional biochemical ATPase assay.

However, for the investigation of membrane proteins by means of ssNMR, the amount of available protein, the quality of the sample preparation, the concentration of the measured sample and the careful reconstitution present major bottlenecks. These can be overcome by careful screens leading to the desired result of a reconstituted and functionally intact full-length protein. Here, we show that sufficient sample amounts of LmrA can be prepared and reconstituted using an optimised protocol so that ATP hydrolysis can be followed by real time ^{31}P magic angle spinning (MAS) NMR. To slow down ATP hydrolysis, we have used LmrA dK388, which has a lysine deletion in the Walker A domain of the NBDs. In biochemical assays such a mutant is often used as a negative control [27], whereas for our purposes this mutant is ideal, since its slow ATP turnover rate makes time-resolved NMR detection at high protein concentrations easier. Using ^{31}P-MAS NMR, we were able to determine the rates of the formation of ADP from ATP by following variations in the α, β and γ phosphate signals. These rates are discussed in the context of data from conventional biochemical assays.

2. Materials and methods

2.1. Materials

Difco M17 Medium was obtained from BD, Sparks, membrane domain (MD); *n*-dodecyl-β-D-maltoside (DDM) and TritonX-100 from Applichem; Ni^{2+}-nitriloacetic acid (NI-NTA) resin from Qiagen, Inc.; BioBeads SM2 from Bio-Rad Laboratories Inc.; 1-palmitoyl-2-oleoyl-*sn*-glycero-3-phosphocholine (POPC) and 1-palmitoyl-2-oleoyl-*sn*-glycero-3-[phospho-*rac*-(1-glycerol)] (POPG) from Avanti Polar Lipids, Alabaster, AL. Adenosinetriphosphate was obtained from Sigma. All other chemicals were of analytical grade or better.

2.2. Bacterial strains and growth conditions

Lactococcus lactis strain NZ9700 was used as a nisin producing strain. *L. lactis* strain NZ9000 Δ*lmrA*Δ*lmrCD* with plasmids pNHLmrA-dK388 [27] or pNHLmrA-MD [27,28] was used for expression of membrane protein. Twenty millilitres of cells per litre of main culture were grown without shaking at 30 °C overnight in M17 medium with 0.5% glucose

and 5 μg/mL chloramphenicol. These cells were used to start main cultures (16 L) to grow at 30 °C without shaking to an OD$_{660}$ of 0.8. Cells were then induced with 1 mL per litre main culture of the supernatant of a *L. lactis* strain NZ9700 culture after centrifugation. Cells were grown for 2 h and then harvested by centrifugation.

2.3. Sample preparation

Inside-out vesicles were prepared as previously described [29] with slight modifications: 2 mg/mL lysozyme were used for digestion and 25 μg/mL of DNAse were added to the cell suspension after passage through a cell disruptor and the cell suspension was then incubated for further 30 min at 30 °C. Total membrane protein yield was determined with the colourimetric DC Protein Assay (Bio-Rad, Hertfordshire, UK) and detected at 750 nm with a UV-550 Jasco spectrophotometer.

His-tagged protein was solubilized in 50 mM KPi pH8 with 1% DDM, 100 mM NaCl and 10% glycerol over night and then purified as described by [14] but with KPi buffer pH 7.0 instead of Tris–HCl buffer pH 7.0. Pure protein yields were again determined with the DC Protein Assay and verified with SDS–PAGE.

Lipids for reconstitution were weighed to give a 70:30 (w/w) ratio of POPC to POPG and solubilized in chloroform for homogenous mixing. They were then dried overnight and stored frozen until needed. For liposomes, a 4 mg/mL solution of lipids was prepared in 50 mM KPi buffer, pH 7 and extruded (Northern Lipid Extruder) 11 times through a 400 nm filter (Whatman, Maidstone, UK). Liposomes were then destabilized by titration with a 10% TritonX-100 solution and the process was followed by UV–Vis spectroscopy at 540 nm. Destabilized liposomes were combined with eluted protein in a ratio of 150:1 (mol/mol) and incubated for 30 min at room temperature. Biobeads were added to a final concentration of 80 mg/mL and incubated for 2 h at room temperature. Biobeads were then exchanged to yield again a concentration of 80 mg/mL and incubated for 2 h at 4 °C. Biobeads were then exchanged a final time in the above manner and the solution incubated over night at 4 °C. Reconstituted protein was harvested by centrifugation (190 000 × *g*, 40 min, 4 °C) and reconstitution efficiency checked by freeze fracture electron microscopy.

For time resolved NMR data acquisition, liposome pellets containing 15 mg total membrane protein of the reconstituted protein was spun into the NMR rotor at 4 °C as a first step. 20 μL of the precooled ATP solution (100 mM KPi, 100 mM ATP, 10 mM MgCl$_2$, pH 7.0) were then pipetted into the rotor. The rotor was quickly closed with a top insert, screw and cap and then vortexed. The sample was then inserted into the prewarmed spectrometer and measurement began within 1 min of start of reaction. After NMR measurements, samples were measured once more by freeze fracture electron microscopy.

2.4. Activity assay

ATPase activity of purified protein was determined using a linked assay: pyruvate kinase turns ADP generated by LmrA back into ATP by producing pyruvate from phosphoenolpyruvate. Pyruvate is used by the second enzyme, lactate dehydrogenase, to yield lactate under the consumption of NADH. The turnover of NADH is observed spectroscopically and can be related to the LmrA ATP activity. The assay was carried out as described previously [26] but without β-octyl glucoside, dimyristoylphosphatidylcholine, EGTA and *sn*-1,2-dihexanoylglycerol. 100 μL assay buffer containing 25 mM PIPES, pH 6.8, 50 mM LiCl, 0.1 mM EDTA, 0.5 mM NADH, 3 mM ATP, 15 mM MgCl$_2$, 1 mM phosphoenolpyruvate and 5 μL of pyruvate kinase (200 U/mg) and lactate dehydrogenase (550 U/mg) (both Roche, mixed at a ratio 100:72.7) were incubated at 30 °C for 5 min. LmrA dK388 was then mixed with the assay buffer and NADH decrease was monitored at 340 nm.

2.5. Electron microscopy

Freeze-fracture replicas produced in the freeze-fracture unit BAF 060 (Bal-TEC Inc., Principality of Liechtenstein) were analyzed in an EM208S electron microscope (FEI Company).

2.6. ssNMR

All experiments were carried out using a Bruker Avance II 400 MHz Spectrometer with a 4 mm MAS DVT Triple Resonance probe in double resonance mode. Direct polarization of ^{31}P was carried out at 161.923 MHz with a pulse length of 6.5 μs. Protons were decoupled

during acquisition with 70 kHz using spinal64 [30]. All experiments were carried out at 290 K. All spectra were processed using Topspin 2.0 (Bruker, Karlsruhe, Germany). Spectra were referenced with respect to phosphoric acid.

3. Results and discussion

In order to carry out ssNMR experiments on ABC transporters, it is necessary to find conditions under which large amounts of the isotope labelled protein can be fully functionally prepared at high concentration within the lipid bilayer. Mason et al. already showed that isotopic labelling is possible with *L. lactis* as an overexpression host [31].

For biochemical analysis, LmrA is usually reconstituted at a ratio of approximately 1:100 (w/w) (1:~8000 (mol:mol) protein:lipid) [29]. For ssNMR measurements however, a much higher protein density needs to be achieved. In a previous paper, we have shown that LmrA could be overexpressed in *L. lactis* and then reconstituted into *E. coli* full lipid extract with a molar ratio of approximately 1:250 (protein:lipid) [31]. Here, we have further lowered the reconstitution ratio down to 1:150 (mol/mol) which allows us to accommodate more protein in the limited volume of a MAS NMR sample rotor. Additionally, we have changed the reconstitution protocol from *E. coli* full lipid extract to a mixture of the synthetic lipids POPC and POPG (70:30, w/w) which did allow higher reproducibility between preparations. The successful homogenous reconstitution was examined with freeze fracture electron microscopy before and after MAS NMR experiments; no aggregates were detected (Fig. 1), which shows that spinning the sample at 10 kHz does not lead to aggregation of the sample during measurement. This high reconstitution efficiency enabled us to fit 15 mg of purified and reconstituted protein into the MAS rotor volume of about 70 µL.

Using these conditions, we tried to observe ATP activity directly by ^{31}P-MAS NMR. For this purpose, samples of purified and reconstituted LmrA with a deletion in the Walker A domain (LmrAdK388) have been prepared. This mutant shows a much slower ATP hydrolysis and is therefore better suited for real time NMR experiments than the wild type protein: Due to the limited sample volume of ca. 70 µL only a limited amount of ATP can be added which will be hydrolysed during the experiment. The longer this takes, the better will be the signal-to-noise and the time resolution of the MAS NMR experiments. An earlier study from our lab by Mason et al has shown that reconstituted LmrA has a basal activity of 47 nmol Pi/min∗mg [31] which indicates that the ATPase activity of LmrAdK388 according to our data is about 4–6% of the wildtype (see below). Changes in the sample are therefore slow enough to record spectra with a sufficient signal-to-noise ratio and a time resolution of minutes. In a previous study, no ATPase activity of LmrAdK388 was detectible because the amount of protein used was some orders of magnitude lower than here [27].

Reconstituted samples were placed into a MAS rotor, incubated with ATP, transferred quickly into a MAS NMR probehead within the NMR spectrometer and spun up to 10 kHz sample spin rate. The recording of the first FID began 1 min after starting the reaction. Two-hundred and fiftysix FIDs were accumulated resulting in a ^{31}P spectrum every 8.8 min. Representative spectra are shown in Fig. 2. The resonances of all three phosphate atoms Pα, Pβ and Pγ of ATP as well as of the two phosphate atoms Pα and Pβ of ADP are well separated from each other and from the PC/PG lipid resonances. During the time course of the experiment, the intensity
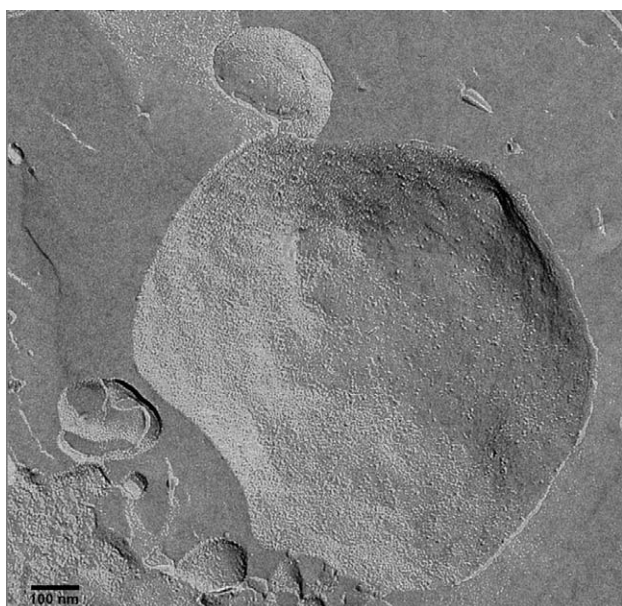

Fig. 1. Electron microscopy freeze fracture image of reconstituted LmrAdK388 in POPC/POPG (7:3 w/w) at a total molar protein:lipid ratio of 1:150 shows a homogeneous protein incorporation into the liposome without apparent aggregation. Images were taken after subjecting the sample to MAS NMR spectroscopy.
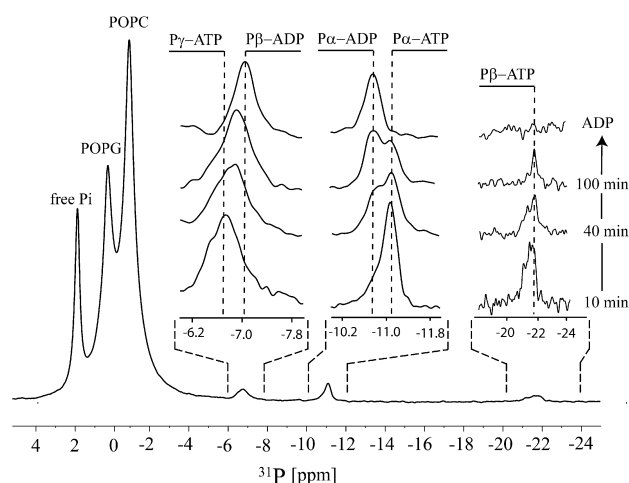

Fig. 2. A series ^{31}P-MAS NMR spectra of LmrA dK388 reconstituted in POPC/POPG in KPi buffer were recorded after adding ATP. The reduced catalytic activity of the dk388 mutant allows directly following ATP hydrolysis in real time: The signal of Pα-ATP at −11.1 ppm decays with time and reappears at −10.8 ppm as Pα-ADP (inset middle). The same signal decay is observed for Pβ-ATP at −21.8 ppm (inset right). The terminal Pγ-ATP and Pβ-ADP resonances cannot be resolved and overlap with a peak maximum apparently shifting from −6.7 ppm to −7.0 ppm (inset left). For comparison, spectra of an identical sample containing ADP only are shown on top of each inset. Spectra were acquired at 290 K, at ^{31}P Larmor frequency of 160 MHz using ^{1}H decoupling, rotating the sample at 10 kHz. For each spectrum, 256 scans were accumulated giving a time resolution of 8.8 min.

Pα-ATP at −11.1 ppm decreases while Pα-ADP at −10.8 ppm increases. Similarly, at −21.8 ppm a decrease of Pβ-ATP is observed. The signal of terminal Pγ-ATP which is cleaved off during hydrolysis cannot be clearly resolved from Pβ-ADP (previously the beta-phosphate of ATP). Both resonances overlap to form a broad peak with a time dependent maximum shifting from −6.7 to −7.0 ppm. These kinetic changes in the ^{31}P spectra are directly caused by the hydrolysis of ATP through LmrAdK388. As a control for ATP hydrolysis, purified and reconstituted LmrA-MD at a molar ratio of 1:150 in POPC:POPG (70:30, w:w), comprising only of transmembrane helices, has been measured under the same conditions. This protein has been shown to act as a secondary multidrug transporter under the influence of a pH gradient, but does not display ATPase activity [28]. The reconstituted truncated membrane protein did not show any changes in the time-resolved ^{31}P spectra, hence no ATP hydrolysis activity (data not shown). This is the first time that a kinetic measurement of an active ABC-transporter has been carried out by MAS NMR. To our knowledge, related measurements on a comparably large system with ssNMR have previously only been carried out with ^{13}C-labelled ATP on Na, K-ATPase (~150 kDa) [32]. In that specific example however, unbound components were filtered out and thus binding rather than kinetics were investigated.

Upon inspecting the data shown in Fig. 2, it seems surprising why ATP hydrolysis is associated with changes in spectral intensities for Pα-ADP, Pα- and Pβ-ATP but with a shift of the peak maximum of the Pγ-ATP/Pβ-ADP resonance. The reason is found in the complex formation of ATP and ADP with Mg^{2+}, which has an ion strength and pH dependent effect on the chemical shifts and lineshapes of the terminal phosphate groups [33,34]. For our experimental situation, an initial Mg^{2+}:ATP ratio of 1:10 was found as an optimum in order to fully exploit the volume of the rotor which causes a characteristic lineshape (supporting information, Fig. S1). With ongoing ATP hydrolysis, the peak for Pγ-ATP becomes smaller and the ATP:Mg^{2+} ratio decreases. At the same time the intensity of Pβ-ADP increases and also the ADP:Mg^{2+} ratio increases with subsequent chemical shift changes. Both peaks overlap which results in an apparently shifting peak maximum.

A quantitative analysis of the time-resolved ^{31}P-MAS NMR spectra is shown in Fig. 3. The signal intensities of Pα-ATP, Pα-ADP and Pβ-ATP can be described with a single exponential function. As one would expect, very similar rate constants, given in the legend to Fig. 3, have been obtained (average 5.5×10^{-4} s^{-1}). The chemical shift changes of the Pγ-ATP/Pβ-ADP peak maximum can also be described empirically by an exponential function with a rate constant similar to the intensity changes of the other phosphate groups.

In order to compare the observed rate constant with conventionally obtained data for ATPase activity, we have to consider one important difference between both approaches: In the enzyme coupled biochemical assay used here, the amount of ATP remains constant during the reaction and in excess of ADP because pyruvate kinase turns ADP generated by LmrA back into ATP (see Section 2). During the NMR experiment, the amount of ATP decreases exponentially. To make these data comparable, we have analyzed the exponential time traces for Pα- and Pβ-ATP (Fig. 3a and b) close to $t = 0$ when ATP is still in excess of ADP. Close to zero, these traces have been approximated by a linear function using a Taylor series
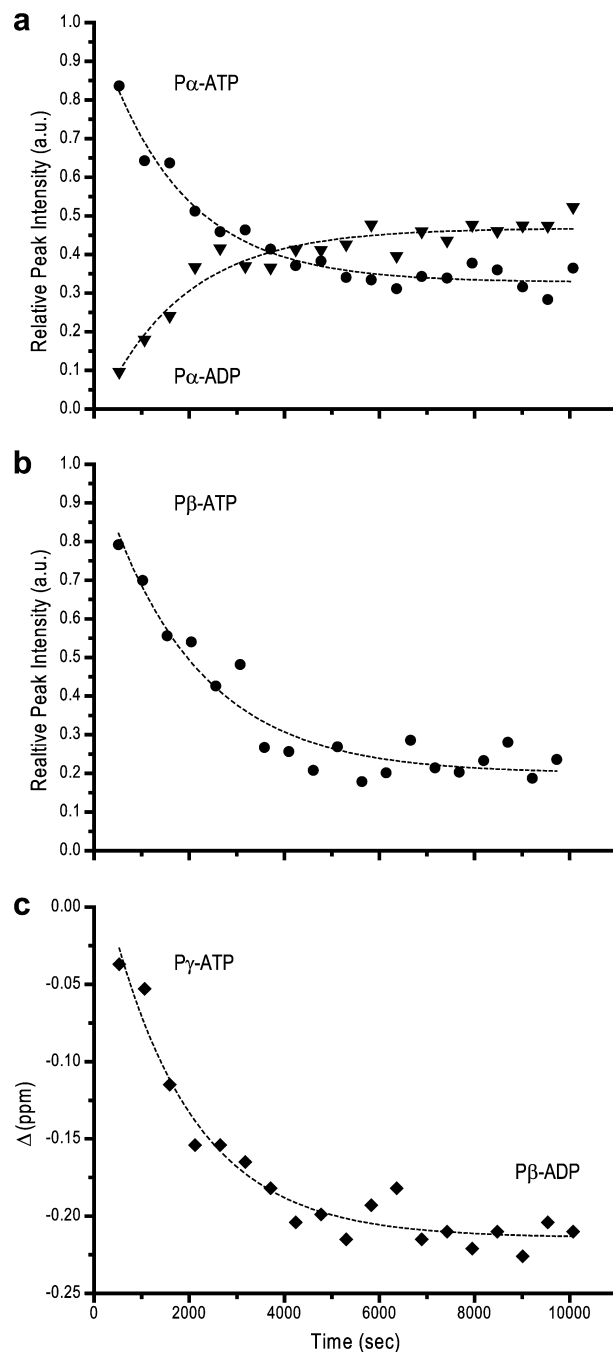

Fig. 3. Time course of ATP hydrolysis obtained from the ^{31}P-MAS NMR spectra shown in Fig. 2. The decay of Pα-ATP and the formation of Pα-ADP can be fitted with a single exponential function with rate constants of $5.8 \pm 0.7 \times 10^{-4}$ s^{-1} and $5.6 \pm 1.0 \times 10^{-4}$ s^{-1}, respectively (a). Pβ-ATP decays exponentially with $5.0 \pm 0.9 \times 10^{-4}$ s^{-1} (b). The peak maximum of the overlapping Pγ-ATP/Pβ-ADP resonance shows a continuous chemical shift change $\Delta = \delta(0) - \delta(t)$ which can also be fitted empirically with a single exponential rate constant of $5.7 \pm 0.7 \times 10^{-4}$ s^{-1} (c).

expansion, which results in an average ATP turnover activity of 3.1 ± 0.5 nmol ATP/min * mg for LmrAdK388. This is in good agreement with our biochemical data which returned 4.1 ± 0.5 nmol ATP/min * mg, showing that kinetic data of a fully active ABC transporter can be obtained by real-time ssNMR. The activity obtained by NMR is slightly lower than

the value obtained biochemically. This could be simply caused by the approximation used here. A reduced NBD accessibility during the MAS NMR experiment could also be considered, because the liposomes are centrifuged onto the inner surface of the MAS rotor. But mixing takes place before sample spinning starts, so this effect is not expected to be significantly large. Sample aggregation due to spinning can also be excluded as the freeze fracture analysis in Fig. 1 was carried out after sample spinning.

4. Conclusion

Our studies show that MAS NMR can be used to probe kinetics of membrane proteins occurring on a time-scale of minutes. It is possible to follow the course of all phosphorylated compounds of an ATP hydrolysis reaction directly and simultaneously with ^{31}P NMR. This holds advantages over biochemical assays and could even be expanded to membrane protein reactions in which also phosphorylated substrates are involved. Additionally, side reactions e.g. ATP/AMP or the reversibility of ATP hydrolysis could be easily monitored.

Further studies will include the effect of substrates on ATP hydrolysis, the use of caged ATP for studies on wildtype LmrA, or to probe the reversibility of such reactions.

It should also be pointed out, that the experimental conditions used here correspond to the requirements of MAS NMR on uniformly ^{13}C and/or ^{15}N or site-directed labelled protein: We were able to show that ssNMR experiments at a high protein:lipid ratio with up to 15 mg of this ABC transporter in its active state can be carried out.

Appendix A. Supplementary data

Supplementary data associated with this article can be found, in the online version, at doi:10.1016/j.febslet.2008.09.033.

References

[1] van Veen, H.W., Callaghan, R., Soceneantu, L., Sardini, A., Konings, W.N. and Higgins, C.F. (1998) A bacterial antibiotic-resistance gene that complements the human multidrug-resistance P-glycoprotein gene. Nature 391, 291–295.

[2] van Veen, H.W., Müller, M., Hioggins, C.F. and Konings, W.N. (2000) The homodimeric ATP-binding cassette transporter LmrA mediates multidrug transport by an alternating two-site (two-cylinder engine) mechanism. EMBO J. 19 (11), 1514–2503.

[3] Schneider, E. and Hunke, S. (1998) ATP-binding cassette (ABC) transport systems: functional and structural aspects of the ATP-hydrolyzing subunits/domains. FEMS Microbiol. Rev. 22, 1–20.

[4] Locher, K.P., Lee, A.T. and Rees, C.C. (2002) The *E. coli* BtuCD structure: a framework for ABC transporter architecture and mechanism. Science 296 (5570), 1091–1098.

[5] Dawson, R.JP. and Locher, K.P. (2006) Structure of a bacterial multidrug ABC transporter. Nature 443, 180–185.

[6] Dawson, R.JP. and Locher, K.P. (2007) Structure of the multidrug ABC transporter Sav1866 from *Staphylococcus aureus* in complex with AMP-PNP. FEBS Lett. 581, 935–938.

[7] Hollenstein, K., Frei, D.C. and Locher, K.P. (2007) Structure of an ABC transporter in complex with its binding protein. Nature 446, 213–216.

[8] Gerber, S., Comellas-Bigler, M., Goetz, B.A. and Locher, K.P. (2008) Structural basis of trans-inhibition in a molybdate/tungstate ABC transporter. Science 321, 246–250.

[9] Pinkett, H.W., Lee, A.T., Lum, P., Locher, K.P. and Rees, D.C. (2007) An inward facing conformation of a putative metal-chelate-type ABC transporter. Science 315, 373–377.

[10] Ward, A., Reyes, C.L., Yu, J., Roth, C.B. and Chang, G. (2007) Flexibility in the ABC transporter MsbA: alternating access with a twist. Proc. Natl. Acad. Sci. USA 104 (48), 19005–19010.

[11] Oldham, M.L., Khare, D., Quiocho, F.A., Davidson, A. and Chen, J. (2007) Crystal structure of a catalytic intermediate of the maltose transporter. Nature 450, 515–522.

[12] Kadaba, N.S., Kaiser, J.T., Johnson, E., Lee, A. and Rees, D.C. (2008) The high-affinity *E. coli* methionine ABC transporter: structure and allosteric regulation. Science 321, 250–253.

[13] Oswald, C., Holland, B.I. and Schmitt, L. (2006) The motor domains of ABC transporters – what can structures tell us? Naunyn-Schmiedeberg's Arch. Pharmacol. 372, 385–399.

[14] Siarheyeva, A., Lopez, J.J., Lehner, I., Hellmich, U.A., van Veen, H.W. and Glaubitz, C. (2007) Probing the molecular dynamics of the ABC multidrug transporter LmrA by deuterium solid-state nuclear magnetic resonance. Biochemistry 46, 3075–3083.

[15] Lehner, I., Basting, D., Meyer, B., Haase, W., Manolikas, T., Kaiser, C., Karas, M. and Glaubitz, C. (2008) The key residue for substrate transport (Glu 14) in the EmrE dimer is asymmetric. J. Biol. Chem. 283 (6), 3281–3288.

[16] Patching, S.G., Henderson, P.J.F., Herbert, R.B. and Middleton, D.A. (2008) Solid-state NMR Spectroscopy detects interactions between tryptophan residues of the *E. coli* sugar transporter GalP and the alpha-anomer of the D-glucose substrate. J. Am. Chem. Soc. 130, 1236–1244.

[17] Placzek, W.J., Almeida, M.S. and Wüthrich, K. (2007) NMR structure and functional characterization of a human cancer-related nucleoside triphosphatase. J. Mol. Biol. 367, 788–801.

[18] Ugurbil, K., Rottenberg, H., Glynn, P. and Shulman, R.G. (1978) 31P nuclear magnetic resonance studies of bioenergetics and glycolysis in anaerobic Escherichia coli cells. Proc. Natl. Acad. Sci. USA 55, 2244–2248.

[19] Kemp, G.J., Meyerspeer, M. and Moser, E. (2007) Absolute quantification of phosphorous metabolite concentrations in human muscle in vivo by ^{31}P MRS: a quantitative review. NMR Biomed. 20, 555–565.

[20] Brown, T.R., Ugurbil, K. and Shulman, R.G. (1977) 31P nuclear magnetic resonance measurements of ATPase kinetics in aerobic Escherichia coli cells. Proc. Natl. Acad. Sci. USA 74, 5551–5553.

[21] Brune, M., Hunter, J.L., Corrie, J.E.T. and Webb, M.R. (1994) Direct, Real-Time measurement of rapid inorganic phosphate release using a novel fluorescent probe and its application to actomyosin subfragment 1 ATPase. Biochemistry 33, 8262–8271.

[22] He, Z.-H., Chillingworth, R.K., Brune, M., Corrie, J.E.T., Trentham, D.R., Webb, M.R. and Ferenczi, M.A. (1997) ATPase kinetics on activation of rabbit and frog permeabilized isometric muscle fibers: a real time phosphate assay. J. Physiol. 501, 125–148.

[23] Chan, K.-M., Delfert, D. and Junger, K.D. (1986) A direct colorimetric assay for Ca^{2+}-stimulated ATPase activity. Anal. Biochem. 157, 375–380.

[24] Janvilisri, T., Venter, H., Shahi, S., Reuter, G., Balakrishnan, L. and van Veen, H.W. (2003) Sterol transport by the human breast cancer resistance protein (ABCG2) expressed in *Lactococcus lactis*. J. Biol. Chem. 278 (23), 20645–20651.

[25] Reimann, E.M. and Umfleet, R.A. (1978) Selective precipitation of ^{32}Pi onto filter papers. Application to ATPase and cyclic AMP phosphodiesterase determination. Biochim. Biophys. Acta 523 (2), :516–521.

[26] Badola, P. and Sanders II, C.R. (1997) *Escherichia coli* diacyl-glycerol kinase is an evolutionary optimized membrane enzyme and catalyzes direct phosphoryl transfer. J. Biol. Chem. 272 (39), 24176–24182.

[27] Venter, H., Velamakanni, s., Balakrishnan, L. and van Veen, H.W. (2007) On the energy-dependence of Hoechst 33342

transport by the ABC-transporter LmrA. Biochem. Pharmacol. 75 (4), 866–874.

[28] Venter, H., Shilling, R.A., Velamakanni, S., Balakrishnan, L. and van Veen, H.W. (2003) An ABC-transporter with a secondary-active multidrug translocator domain. Nature 426, 866–870.

[29] Margolles, A., Putmann, M., van Veen, H.W. and Konings, W.N. (1999) The purified and functionally reconstituted multidrug transporter LmrA of *Lactococcus lactis* mediates the transbilayer movement of specific fluorescent phospholipds. Biochemistry 38, 16298–16306.

[30] Fung, B.M., Khitrin, A.K. and Ermolaev, K. (2000) An improved broadband decoupling sequence for liquid crystals and solids. J. Magn. Reson. 142, 97–101.

[31] Mason, J., Siarheyeva, A., Haase, W., Lorch, M., van Veen, H.W. and Glaubitz, C. (2004) Amino acid type selective isotope labeling of the multidrug ABC transporter LmrA for solid-state NMR studies. FEBS Lett. 568, 117–121.

[32] Middleton, D.A., Jakobsen, L.O. and Esmann, M. (2006) Detection of nucleotide binding to Na,K-ATPase in an aqueous membrane suspension by ^{13}C cross-polarization magic-angle spinning NMR spectroscopy. FEBS Lett. 580, 6685–6689.

[33] Cohn, M. and Hughes, T.R. (1962) Nuclear magnetic resonance spectra of adenosine di- and tri-phosphate – II: effect of complexing with divalent metal ions. J. Biol. Chem. 237 (1), 176–181.

[34] Gupta, R.K. and Moore, R.M. (1980) ^{31}P NMR studies of intracellular free Mg^{2+} in intact frog skeletal muscle. J. Biol. Chem. 255 (9), 3987–3993.